Manuscript

Exposure enhanced photoluminescence of $CdS_{0.9}Se_{0.1}$ quantum dots embedded in spin-coated $Ge_{25}S_{75}$ thin films

Stanislav Slang,†[a] Liudmila Loghina,†[a] Karel Palka, *[b,a] and Miroslav Vlcek[a]

Semiconductor quantum dots (QDs) are well known photoluminescent materials. Their potential practical applications depend on their physico-chemical and luminescent properties and also on properties of hosting material. To ensure that QDs retain their photoluminescence during preparation of suitable solid composite form, the solution based casting techniques with deposition at lower temperatures are usually used. In our work, we have doped inorganic non-toxic $Ge_{25}S_{75}$ chalcogenide glass matrix with synthetized $CdS_{0.9}Se_{0.1}$ QDs and prepared thin films by solution based spin-coating technique. In comparison with commonly used polymers the $Ge_{25}S_{75}$ chalcogenide glass thin films possess high refractive index and wide VIS-NIR-MIR optical transparent region. We also report on the phenomenon of significant UV exposure induced increase of doped thin films photoluminescence intensity which can be exploited in local photo-induced photoluminescence enhancement of doped chalcogenide glass thin films.

Introduction

Semiconductor quantum dots (QDs) have attracted a great deal of interests due to their unique properties.[1-4] The QDs exhibit size-dependent characteristics and they often possess novel electronic, magnetic, optical, chemical, and mechanical properties that cannot be obtained in their bulk counterparts.[5,6] QDs with careful functionalization have been widely used for imaging and sensing [7] or tracking particles and cells [8] in biology and medicine. Blue- and green-light emitting QDs with high photoluminescent quantum yield (PL QY) and pure emission color are critical element for the application of solid state light emitting diodes (LEDs) and lasers.[9] For this broad class of applications, the Cd-based chalcogenides (this term generally refers to sulfur, selenium and tellurium) QDs are regarded to be promising materials.

In the past two decades, significant progress has been made in synthesis of QDs with uniform size, high PL QYs and narrow emission spectra.[10,11] Optimization of QDs synthesis was carried out by systematic changing the reaction conditions including the effect of type of solvent,[12] form of surfactant,[13] precursor form [14] and reaction temperature [15] in order to increase the QY and monodispersity.

Completely different group of chalcogenides are amorphous chalcogenide glasses (ChGs). They are semiconductors with high refractive index and wide IR transparency window.[16-20] ChGs are frequently used in form of bulk glasses (IR optical elements such as lenses, windows etc.) [16,17,21] or their amorphous thin films (optical recording discs, diffractive optical elements, planar waveguides, high resolution photoresists, etc.).[16-20] Metastability of ChGs often results in their sensitivity to various types of irradiation.[16,17,22,23] ChG thin films are usually deposited by physical vapor deposition techniques (e.g. vacuum thermal evaporation, laser ablation, etc.).[16-20] Alternatively, ChGs thin films can be also deposited by solution based deposition techniques, which exploits the solubility of ChGs in volatile organic amines.[24-27] Laboratory scale deposition techniques

(such as spin-coating or dip-coating) have been proven suitable for basic material research.[24-27] ChGs thin films were also successfully deposited from their solutions by electrospray [28] or spiral bar-coating [29] techniques which opens the possibility for their potential mass production by other coating techniques without the need for high vacuum equipment (contrary to the physical vapor deposition methods). The major disadvantage of ChG thin films deposited from solutions is organic residuals content, which can be limiting for some IR optical applications. However, organic residuals content can be significantly reduced by proper post-deposition thermal treatment.[30,31]

Organic polymers are typically used as a host matrix for PL QDs.[32-34] Previous results proved that spin-coated ChG thin films can be also used as host matrix for QDs.[35,36] The usage of ChG host matrix can be advantageous because ChGs possess higher refractive index and wider VIS-NIR-MIR transparent region in comparison with organic polymers.[37-39] In this work, we report on a) "one pot" preparation and characterization of highly PL $CdS_{0.9}Se_{0.1}$ nanoparticles b) and their usage for doping of $Ge_{25}S_{75}$ ChG solution. The $Ge_{25}S_{75}$ ChG is non-toxic and the thin films were successfully deposited by spin-coating technique only recently.[31] The doped $Ge_{25}S_{75}$ thin films deposited by spin-coating technique were of good optical quality, well transparent in VIS and NIR and maintained PL of the QDs. The structural changes in structure of doped spin-coated thin films were induced by UV lamp light exposure. Significant enhancement of thin films PL intensity was observed after illumination and we have also proposed possible mechanism of this phenomenon.

Experimental

Synthesis and isolation of $CdS_{0.9}Se_{0.1}$ nanoparticles

The $CdS_{0.9}Se_{0.1}$ crystalline quantum dots (QDs) were synthetized using cadmium oxide (CdO 99,99 %, Sigma Aldrich), selenium (Se 99,999 %, abcr GmbH & Co. KG), sulfur (S 99,999 %, Sigma Aldrich), trioctylphosphine (TOP, 97 %, Sigma Aldrich), 1-octadecene (ODE, 90 %, Sigma Aldrich) and oleic acid (OA, 90 %,

Sigma Aldrich) precursors. The n-hexane, methanol, toluene, chloroform and acetone solvents (Fisher Scientific) were used for isolation and purification of prepared nanoparticles. Air and/or moisture sensitive chemicals were handled in Ar atmosphere. The reactions were carried out in a standard Schlenk line apparatus under inert Ar atmosphere as well.

The S precursor solution (1 M), containing 0.32 g of S, 5 mL of TOP and 5 mL of ODE, was prepared under an Ar atmosphere; the solution was permanently stirred at 50°C until complete dissolution of S. The Se precursor solution (1 M), containing 0.79 g of Se, 5 mL of TOP and 5 mL of ODE, was prepared under an Ar atmosphere at 100 °C and permanent stirring.

$CdS_{0.9}Se_{0.1}$ QDs were synthesized using a hot-injection method based on the CdSe synthesis developed by Cooper et al. [40] This method was modified according to the synthesized composition. In a 50 mL Schlenk flask 0.385 g CdO (0.003 mol) was suspended with 3.56 mL OA (0.012 mol) in 15 mL ODE. Using a Schlenk line and vacuum pump, the mixture was degassed at room temperature for 20 min, then at 100 °C 20 min and then finally heated up to 280 °C to form clear solution. The mixture of S (2.7 mL, 0.0027 mol of S) and Se (0.3 mL, 0.0003 mol of Se) precursor solutions was injected instantaneously into the heated CdO solution using an air free injection procedure. After injection, the temperature of reaction mixture was decreased to 240 °C and kept at this temperature for growing of QDs. The size of QDs was monitored using UV-VIS spectroscopy and photoluminescence (PL) measurements by taking out of aliquots at different time intervals. The aliquots were dispersed in toluene for spectroscopic measurements.

The crude reaction mixture was dissolved in 50 mL of n-hexane and washed three times with methanol to remove unreacted precursors. The hexane solution was diluted by 50 mL of chloroform. Finally, the QDs were precipitated by adding anhydrous acetone. Precipitated QDs were separated in a centrifuge (Gusto Mini Centrifuge, Fisherbrand) by spinning down at 10,000 rpm for 7 min. For purification of QDs this procedure was repeated 3 times. Separated pure QDs were dried in vacuum for 4 hours. The weight of pure $CdS_{0.9}Se_{0.1}$ QDs was 0.521 g.

The UV-VIS absorbance spectra of prepared aliquot QDs solutions in toluene were measured using UV-VIS-NIR optical spectrometer Shimadzu UV3600 (Shimadzu) in spectral region 330–650 nm. The PL measurements were performed using PTI QuantaMaster 400 (Horiba) steady state spectrofluorometer in spectral range 390–700 nm using excitation wavelength λ = 375 nm. X-Ray diffraction measurements (XRD) of dried QDs were performed using Bruker D8 advance Diffractometer with Cu-Kα radiation. Data were recorded across a 2ϑ range of 20-65° with a step size of 0.05°.

In order to verify the shape and diameter of prepared QDs, the particles were deposited onto carbon hole membrane copper grid and HR-TEM images were taken on a FEI Titan Themis 60 (FEI) high resolution transmission electron microscope at acceleration voltage 300 kV.

Deposition and characterization of doped $Ge_{25}S_{75}$ thin films

The source $Ge_{25}S_{75}$ bulk glass was synthetized using standard melt-quenching method. High purity 5N elements were loaded into the quartz ampule in appropriate amounts and sealed under vacuum (~10^{-3} Pa). The glass synthesis was performed in rocking tube furnace at 950 °C for 72 hours. The ampule with melted glass was quenched in cold water.

Prepared $Ge_{25}S_{75}$ bulk glass was powdered in agate bowl and dissolved in n-butylamine solvent (BA) with concentration 0.0804 g of glass powder per 1 mL of BA. The vacuum dried $CdS_{0.9}Se_{0.1}$ QDs were dispersed in chloroform with concentration 0.02 g of QDs per 1 mL of chloroform. The 1.4 mL of $Ge_{25}S_{75}$ glass solution was mixed with 0.1 mL of QDs solution right before thin film deposition (0.075 g $Ge_{25}S_{75}$ and 0.0013 g $CdS_{0.9}Se_{0.1}$ QDs per 1 ml of final solution). Prepared solution of $Ge_{25}S_{75}$ ChG and $CdS_{0.9}Se_{0.1}$ QDs was clear without any precipitate. The blank (undoped) glass solution was prepared by mixing 1.4 mL of $Ge_{25}S_{75}$ glass solution with 0.1 mL of pure chloroform. Doped and undoped ChG thin films were deposited using spin-coating method on spin-coater SC110 (Best Tools) by pipetting 100 µl of solution onto soda-lime glass substrates rotating at 2000 rpm yielding thin films of good optical quality. The thin films were stabilized by annealing at 60 °C for 20 minutes on a hot plate immediately after deposition (hereinafter referred as as-prepared thin films). Deposited samples were stored in dry and dark environment.

Samples of as-prepared thin films were annealed at temperatures 90, 120, 150, 180 and 210 °C for 60 min on precise annealing table (Conbrio) inside argon filled annealing chamber. In order to examine the effect of irradiation on doped spin-coated thin films the samples were exposed to UV lamp light (365 nm, 137 mW·cm^{-2}) in argon atmosphere for 60 min.

Transmission spectra of studied thin films were measured using UV-VIS-NIR optical spectrometer (Shimadzu UV3600) in spectral region 190–2000 nm. The spectra measurements were always performed on four samples with the same treatment. The elemental compositions of the as-prepared, annealed and exposed thin films together with vacuum dried $CdS_{0.9}Se_{0.1}$ QDs were analyzed by energy dispersive x-ray microanalysis method (EDS) using scanning electron microscope (LYRA 3, Tescan, Czech Republic) equipped with EDS analyzer Aztec X-Max 20 (Oxford Instruments) at acceleration voltage 5 kV. The PL measurements of doped thin films were performed using QuantaMaster 400 steady state spectrofluorometer in spectral range 410–620 nm using excitation wavelength λ = 400 nm (5 nm slit), which was not absorbed by $Ge_{25}S_{75}$ thin film matrix.

Results and Discussion

Crystallographic structure of vacuum dried $CdS_{0.9}Se_{0.1}$ QDs powder was determined by XRD (Figure 1). All measured diffractions can be assigned to the standard pattern of the face centered cubic phase with space group F-43m, which suggests previously proposed mechanism of low temperature crystal growth.[41-43] Calculated cell parameter a of studied QDs is 5.878(4) Å. The low width of observed diffraction peaks suggests nanosize QDs. The mean crystalline domain size D of $CdS_{0.9}Se_{0.1}$ QDs was calculated using Scherrer equation [44]:

$$D = (K \lambda) / (\beta \cos\theta)$$

where λ is wavelength of X-ray beam (0.15406 nm), β is full width at half maximum (FWHM) of diffraction peak at 2θ and θ is the Bragg diffraction angle. K is a shape factor which value is dependent on shape of crystallites. Considering the Gaussian shape of XRD peak, the parameter K is 0.9. The average crystalline domain size of $CdS_{0.9}Se_{0.1}$ QDs sample is 2.93 nm.
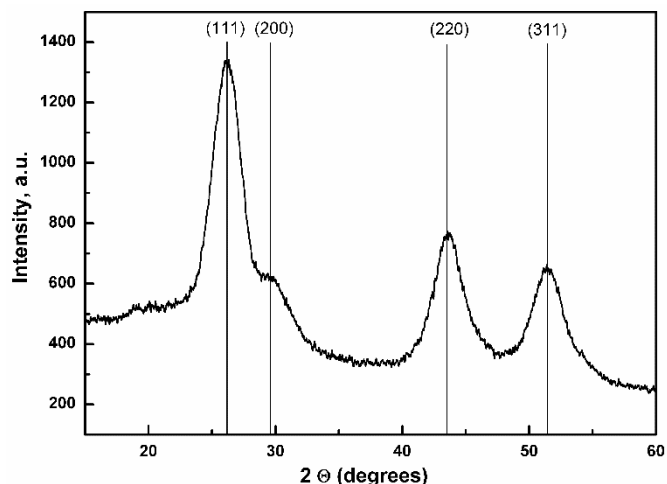

Fig. 1 XRD pattern of $CdS_{0.9}Se_{0.1}$ crystalline nanoparticles.

The HR-TEM microscope was used to study the shape and diameter of prepared $CdS_{0.9}Se_{0.1}$ QDs. Measured TEM scans (Figure 2) confirm that QDs have spherical shape and narrow size distribution. Using the image analysis method, the average QDs size was determined at 3.98 ± 0.39 nm. The difference from QDs diameter obtained by Scherrer formula (2.93 nm) can be attributed to model's neglection of surface effects which starts to be more eminent in nano-diameters. The well-developed lattice fringes (inset of Fig. 2) indicate a good crystallinity of studied $CdS_{0.9}Se_{0.1}$ QDs sample.

The elemental composition of prepared QDs powder was studied by EDS technique. The results confirmed $Cd_{54.4}S_{39.9}Se_{5.7}$ QDs composition, which slightly differs from planned $Cd_{50}S_{45}Se_5$ (~ $CdS_{0.9}Se_{0.1}$) composition probably due to different reactivity of used precursors.[45] The EDS spectra also confirmed the presence of carbon and oxygen, which can be explained by presence of oleic acid capping shell.
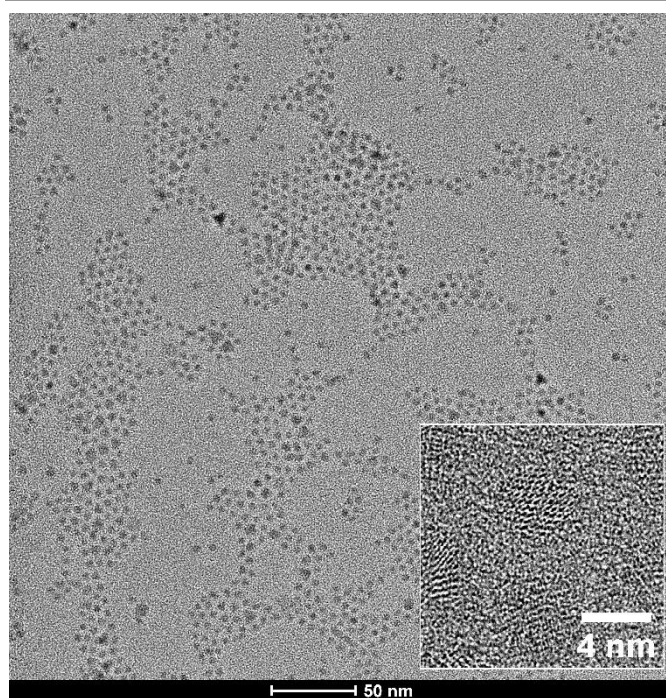

Fig. 2 The HR-TEM image of $CdS_{0.9}Se_{0.1}$ crystalline nanoparticles.

UV-VIS absorption spectra of aliquot QDs samples taken from reaction mixture at various times since the start of reaction are presented in Figure 3. With increasing reaction time the absorption peak maxima are shifting towards longer wavelengths which can be explained by increasing of QDs size.
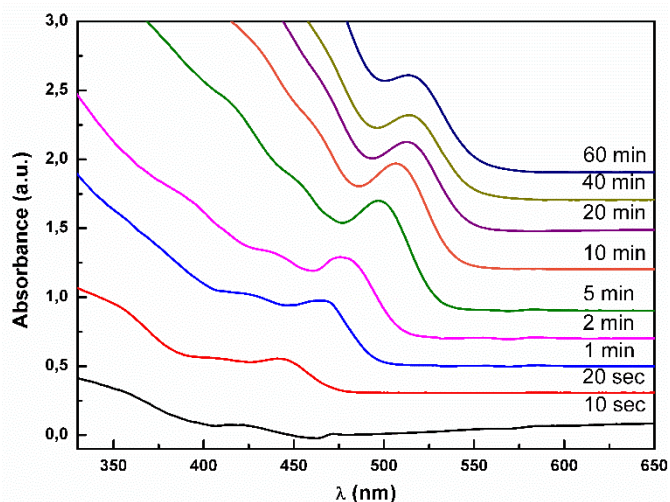

Fig. 3 Chronological evolution of absorption spectra of $CdS_{0.9}Se_{0.1}$ QDs.

Accordingly, the position of their photoluminescence (PL) peaks is also shifting towards higher wavelengths (Figure 4 – A). The PL peak position is changing from 447 nm for sample taken from reaction mixture at 10 secs to 544 nm for samples taken from reaction mixture at 60 min. The reaction time has also high influence on values of PL peak maximal intensity (Figure 4 – B).
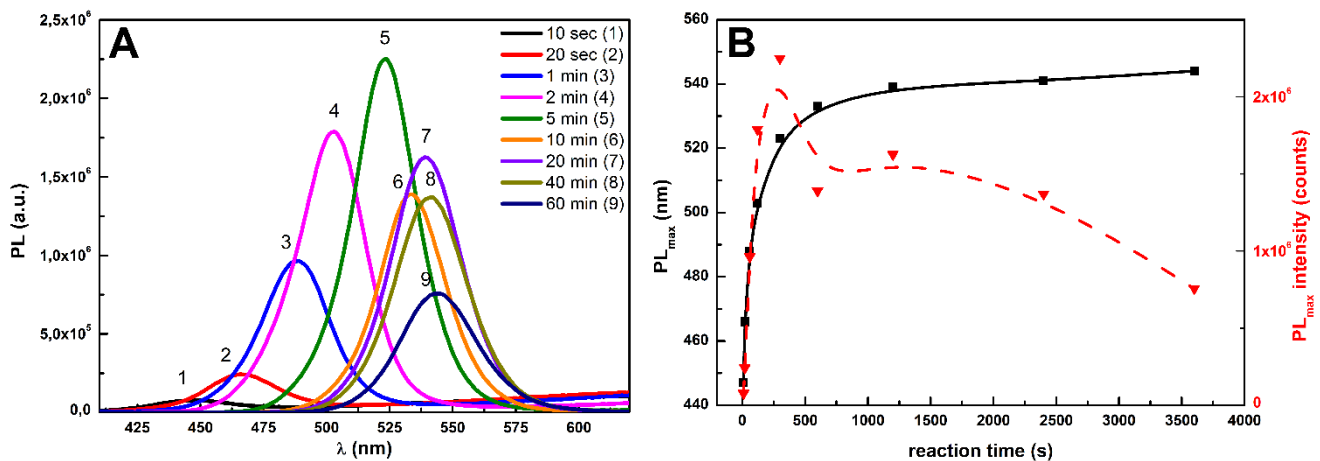
Fig. 4 The evolution of photoluminescence (PL) spectra of $CdS_{0.9}Se_{0.1}$ QDs (A) in dependence on reaction time, dependence of PL maxima position and intensity on reaction time (B).

Their values are significantly increasing up to the reaction time of 5 min. After that, the values of PL intensities are gradually decreasing. The $CdS_{0.9}Se_{0.1}$ QDs prepared at the reaction time of 60 min were chosen for doping of $Ge_{25}S_{75}$ chalcogenide thin films, because their PL band position lies well-inside the transparent region of planned $Ge_{25}S_{75}$ chalcogenide glass matrix.[31]

It was confirmed that $Ge_{25}S_{75}$ chalcogenide glass thin films can be prepared from n-butylamine (BA) solution by spin-coating technique in good optical quality.[31] For doping of $Ge_{25}S_{75}$ chalcogenide glass thin films with prepared $CdS_{0.9}Se_{0.1}$ QDs it is necessary to mix both components without precipitation in mixed solution. Thus, the $CdS_{0.9}Se_{0.1}$ QDs were dispersed in chloroform whose small addition into $BA-Ge_{25}S_{75}$ solution did not induced any observable changes in homogeneity.

The PL spectra of $CdS_{0.9}Se_{0.1}$ QDs (0.005 g / mL) in various solutions are presented in Figure 5. The QDs solution in pure chloroform ($CHCl_3$) has the highest PL intensity with peak maximum at 554 nm which is slightly higher that the peak maximum at 544 nm found in toluene aliquot solution (Figure 4 – B, 3600 s). Small addition of BA into chloroform QDs solution (0.1 mL of BA into 1.4 mL of QDs chloroform solution) significantly decreased PL intensity. When the same volume of $Ge_{25}S_{75}$ or S solution in BA (0.03 g / mL) was mixed with QDs chloroform solution, the PL was practically extinguished. It can be explained by reaction of $CdS_{0.9}Se_{0.1}$ QDs with BA and/or products of $Ge_{25}S_{75}$ chalcogenide glass dissolution in BA. The possible reaction of oleic acid capping agent with basic BA also cannot be excluded. The Ge-S and Ge-Sb-S chalcogenide glasses are dissolving in aliphatic amines and forming ionic compounds of alkyl ammonium germanium sulfide (AAGS) salts.[26,31] Due to the over-stoichiometry of S in $Ge_{25}S_{75}$ bulk glass, the BA chalcogenide glass solution also contain free sulfur fragments, which were also found in BA solutions of S-rich As-S chalcogenide glasses.[25] Those dissolution products and BA

solvent are probably reacting with $CdS_{0.9}Se_{0.1}$ QDs, which is reflected in decrease of their PL intensity.

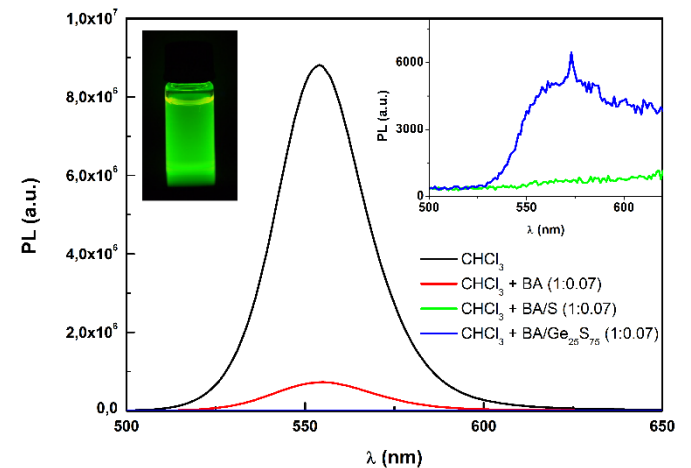**Fig. 5** PL spectra of $CdS_{0.9}Se_{0.1}$ QDs in chloroform ($CHCl_3$) with addition of various solutions. The left inset photo shows the $CdS_{0.9}Se_{0.1}$ QDs - $CHCl_3$ solution under UV lamp light.

The $Ge_{25}S_{75}$ solution in BA (1.4 mL) was mixed with $CdS_{0.9}Se_{0.1}$ QDs solution in chloroform (0.1 mL) to yield the concentration of 0.075 g $Ge_{25}S_{75}$ and 0.0013 g $CdS_{0.9}Se_{0.1}$ QDs / mL of final solution. The clear solution without any precipitate was used for spin-coating of doped thin films. To distinguish the effect of chloroform and QDs on properties of deposited thin films, the undoped (blank) thin films were deposited from mixture of $Ge_{25}S_{75}$ solution in BA (1.4 mL) and pure chloroform (0.1 mL). It was confirmed, that spin-coated chalcogenide glass thin films of various compositions can be also photo-sensitive.[30,46,47] Thus, the prepared thin films were also exposed to UV lamp light (365 nm) and the influence of UV exposure on optical properties and PL was studied.
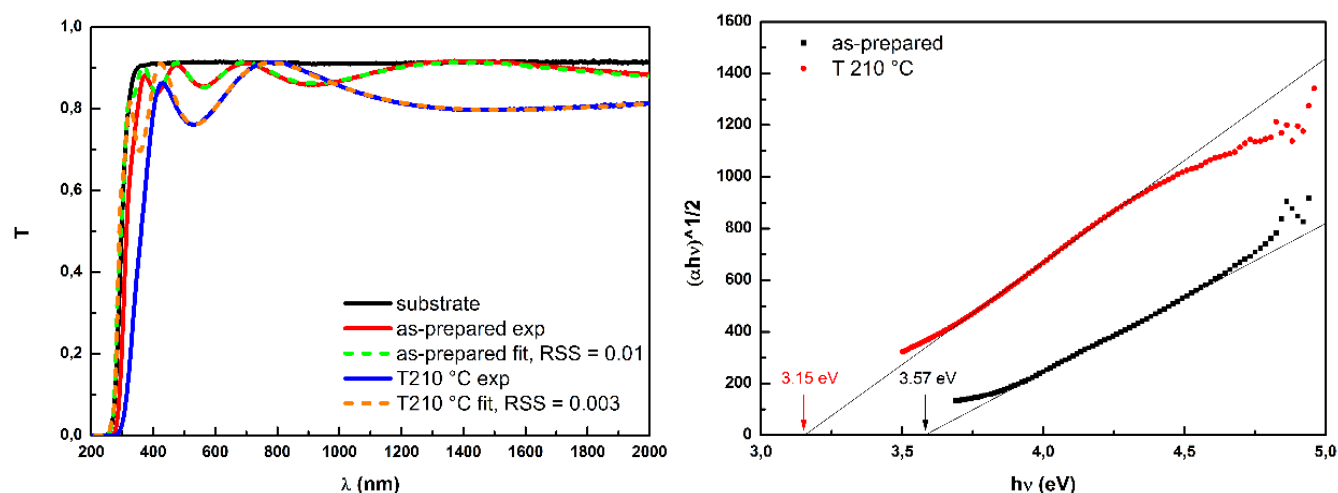
Fig. 6 The measured and fitted transmission spectra (left) and Tauc's plots (right) of as-prepared and annealed spin-coated doped $Ge_{25}S_{75}$ thin films (exp − experimental data, fit − fitted data, RSS − residual sum of squares in fitted transparent region).

The geometrical and optical parameters of prepared blank and doped $Ge_{25}S_{75}$ thin films were calculated by procedure presented in [29,47] based on Swanepoel's model [48] and Wemple-DiDomenico's equation [49] from transmission spectra of studied thin films. Due to the size of used QDs (d ∼ 4 nm) which is significantly smaller than probing wavelengths (d << λ) the measured thin films can be considered homogeneous and thus used model of transmission spectra remains valid. The quality of fit was determined as residual sum of squares (RSS) between fitted and experimental spectrum. The RSS of fitted data didn't exceed the value of 0.04 (within fitted transparent region ∼ 400 - 2000 nm). Provided data of optical parameters and thickness represent the average values of four measurements and the error bars stand for the standard deviation of calculated values. The typical fitted spectrum of as-prepared and annealed thin film together with Tauc's plot [50] are presented in Figure 6.

Figure 7 demonstrates that the thicknesses of all studied samples are significantly decreasing with increasing annealing temperature. Thickness decrease can be explained by thermal decomposition of present AAGS salts connected with releasing of organic solvent residuals and ongoing structural polymerization. Previously it was confirmed that these salts start to decompose at ∼ 120 °C.[31] The decomposition process should be practically completed at 210 °C [31], when the $Ge_{25}S_{75}$ thin film annealed at 210 °C has ∼ 48% of as-prepared thin film thickness. The data also proves that doping and UV exposure treatment have no significant effect on the thickness of studied thin films.

The refractive index n_{1550} (λ = 1550 nm) of all studied samples is increasing with increasing annealing temperature (Figure 8 − A). The refractive index values of blank and $CdS_{0.9}Se_{0.1}$ QDs doped unexposed thin films are nearly identical. Data proved that $Ge_{25}S_{75}$ spin-coated thin films are also photo-sensitive. The refractive index of UV exposed blank and doped thin films annealed at 120 and 150 °C is lower than refractive index of unexposed samples. Values of refractive index of samples annealed at 180 and 210 °C are not influenced by the UV exposure. Thin films annealed above 150 °C are more

structurally polymerized and with significantly decreased content of organic residuals.[31] Thus, the observed photo-sensitivity is probably connected with organic residuals content and level of structural polymerization.[31]
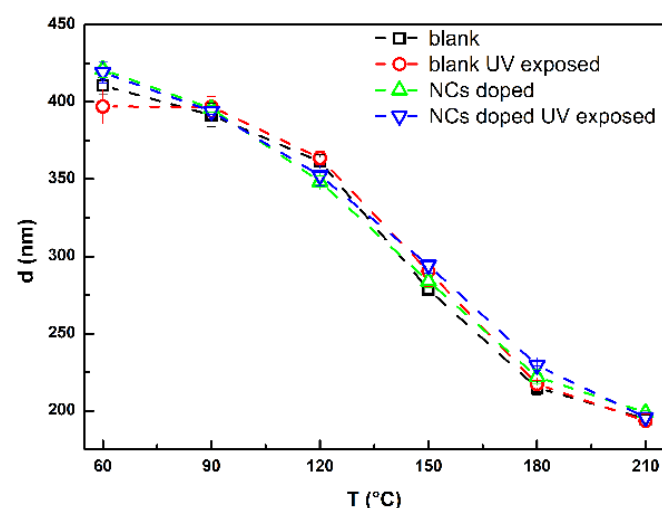

Fig. 7 The thickness of studied blank and doped unexposed and UV exposed $Ge_{25}S_{75}$ thin films in dependence on the annealing temperature.

Contrary to refractive index, the optical bandgap E_g^{opt} of studied thin films is decreasing with increasing annealing temperature – thermo-induced darkening (Figure 8 − B). The data proved that UV exposure and doping have no significant effect on E_g^{opt} of studied thin films. The observed differences are within the experimental error of used evaluation method.

The elemental composition of $Ge_{25}S_{75}$ thin films was studied by EDS analysis. EDS confirmed that as-prepared thin films have composition $Ge_{25.8}S_{74.2}$, which is within EDS margin of error to that of planned nominal composition $Ge_{25}S_{75}$. With increasing annealing temperature, some portion of sulfur is released from thin film matrix leaving S depleted $Ge_{27.9}S_{72.1}$ thin film annealed at 210 °C. The EDS analysis of doped thin films have not confirmed the presence of Cd or Se which would indicate $CdS_{0.9}Se_{0.1}$ QDs content in thin films matrix. It could be explained
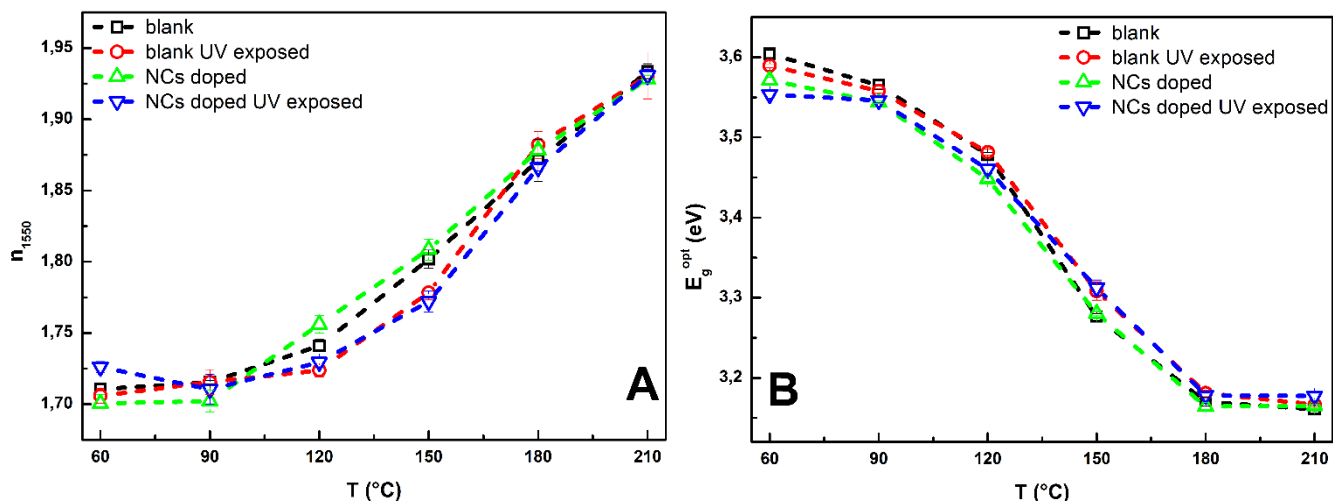
Fig. 8 The refractive index n_{1550} at $\lambda = 1550$ nm (A) and optical bandgap E_g^{opt} (B) of studied blank, doped unexposed and UV exposed $Ge_{25}S_{75}$ thin films in dependence on the annealing temperature

by low concentration of QDs, bellow the detection limit of detector (<0.1 at. %).

The content of organic residuals in thin film matrix was studied using the content of N atoms. BA molecule contains only one N atom and no other sources of N can be expected. Thus, content of N should be equivalent to content of organic BA residuals. Figure 9 demonstrates that the content of organic residuals is decreasing with increasing annealing temperature. The shape of obtained curves is similar to the trend of thermal dependent thickness decrease (Figure 7), which supports the strong connection between thermal induced thickness decrease and releasing of organic residuals from thin film matrix. The doping or UV exposure of studied thin films have no significant effect on the content of organic residuals, with exception of doped sample annealed at 120 °C.
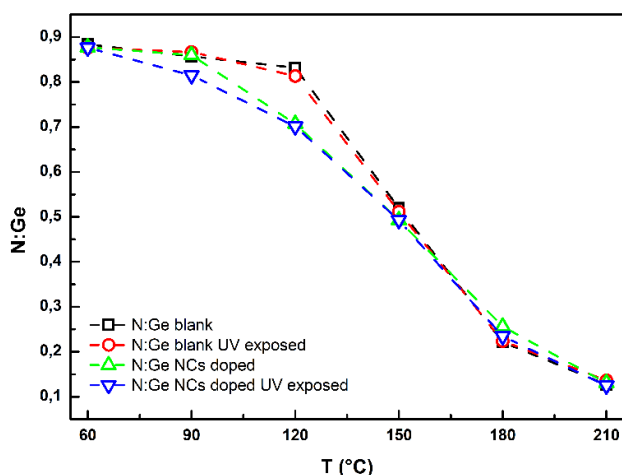

Fig. 9 Dependence of nitrogen/germanium ratio measured by EDS on the annealing temperature.

The PL spectra of studied $Ge_{25}S_{75}$ thin films were recorded using an excitation wavelength 400 nm (~3.1 eV), which should be transmitted by chalcogenide glass matrix (see Fig. 8 - B). The PL spectra confirmed that neither unexposed nor exposed blank

samples have any significant PL in VIS spectral region (Figure 10). Contrary, the unexposed doped thin films exhibit PL at 537 nm. The intensity of observed peaks is significantly decreasing with increasing annealing temperature. Previous results confirmed, that thermo-induced structural changes can be expected in $Ge_{25}S_{75}$ spin-coated thin films. [31] With increasing annealing temperature, the glass matrix of Ge-S spin-coated thin film is more compact and polymerized. Present $CdS_{0.9}Se_{0.1}$ QDs can be also bonded to glass matrix by sulfur bridging atoms, which can result in decrease of QDs PL due to the exciton energy transfer and possible disruption of QDs crystalline lattice. Kovalenko et al. [35] have prepared inorganically functionalized core-shell PbS/CdS QDs with As-S capping agent, which had strong IR PL in As_2S_3 glass matrix. Novak et al. [36] have also successfully doped $Ge_{23}Sb_7S_{70}$ glass matrix with PbS quantum dots and core-shell CdSe/ZnS QDs, but they have obtained well-developed and separated PL peaks only by using the core-shell CdSe/ZnS QDs. Thus, the QDs shell is probably bonded to glass matrix during stabilization annealing, leaving the QDs core protected and their annealed doped chalcogenide thin films are well luminescent.

The UV exposure of $Ge_{25}S_{75}$ doped thin film samples has a strong influence on their PL (Figure 10, 11). The PL intensity values of UV exposed doped thin films are ~3-10 times higher than the values of unexposed doped samples PL. The PL maxima are also slightly shifted to shorter wavelength (530 nm) due to the UV exposure. The UV exposure induced enhancement of pure Zn-Ni-S QDs PL was already reported by Z. Jindal and N. K. Verma.[51] Their QDs were exposed to hard UV light (255 nm) for 24 hours, which induced changes in QDs structural properties resulting in slight increase in PL intensity. Our $Ge_{25}S_{75}$ doped thin films were exposed to 365 nm UV light only for 60 min, but increase in PL intensity is much more significant. Considering our results as well as results published in [35,36], we can assume that observed UV induced increase in PL intensity is probably connected with some structural changes on the boundary between $CdS_{0.9}Se_{0.1}$ QDs and $Ge_{25}S_{75}$ glass matrix.

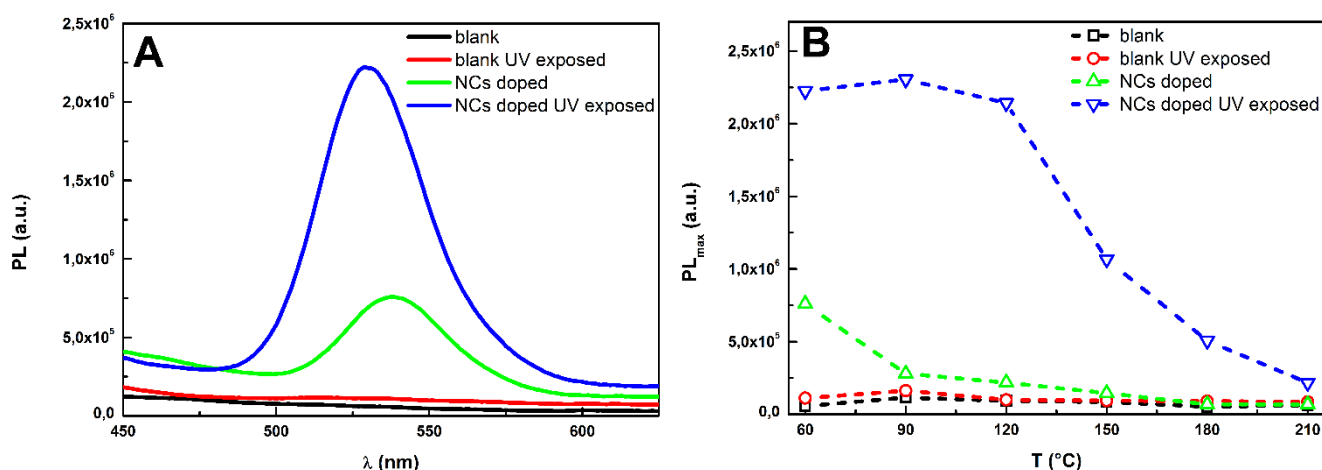**Fig. 10** The PL spectra of blank and doped as-prepared $Ge_{25}S_{75}$ thin films (A) together with PL intensities at PL maxima of treated blank and doped $Ge_{25}S_{75}$ thin films (B)

With increasing annealing temperature of pre-exposed thin films, the QDs are more bonded into the structure of chalcogenide glass thin film and the effect of UV exposure is decreased. The effect of UV lamp light exposure which resulted in such significant increase in films' PL intensity can be exploited in local PL enhancement induced by beam of higher energies whereas the beam of lower energy would only induce the PL without changing of PL intensity.
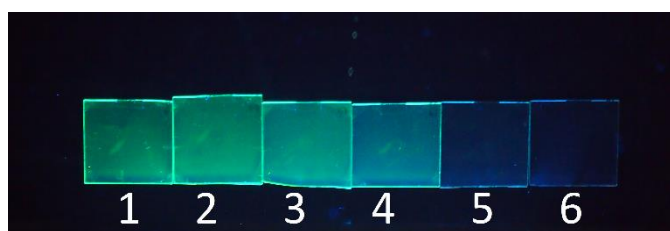

Fig. 11 The $CdS_{0.9}Se_{0.1}$ QDs doped spin-coated $Ge_{25}S_{75}$ thin films after 60 min UV exposure under UV lamp light. 1 – as-prepared thin film, 2 – annealed at 90 °C, 3 – annealed at 120 °C, 4 – annealed at 150 °C, 5 – annealed at 180 °C, 6 – annealed at 210 °C

Although the physico-chemical processes in mixed QDs/glass solution and in doped spin-coated thin films during annealing and exposure are relatively complicated issue we propose one possible interpretation of the presented data. As discussed above, after mixing of $CdS_{0.9}Se_{0.1}$ QDs with $Ge_{25}S_{75}$ BA solution the QDs are bonding with chalcogenide glass fragments. This process is probably accelerated by substitution of oleic acid capping agent with BA molecules.[52] Products of this reaction have no significant PL which can be explained by absence of appropriate protecting QDs shell. After deposition of thin films from prepared solution, the QDs are weakly bonded to as-prepared glass matrix. The structure of thin film and QDs is gradually polymerized with increasing of annealing temperature which further decreases the PL intensity. UV exposure of deposited thin films probably induces releasing of QDs from bonds with glass matrix which significantly increases PL intensity, but the effect of this process depends on thermal pre-history of sample.

Conclusions

The spherical $CdS_{0.9}Se_{0.1}$ semiconductor quantum dots (QDs) with 3.98 ± 0.39 nm in diameter were synthesized using a hot-injection method. The QDs in toluene exhibit an intensive luminescence with narrow PL peak at 544 nm. Vacuum dried QDs were mixed with $Ge_{25}S_{75}$ n-butylamine solution and thin films of specular quality were deposited by spin-coating technique. Data proved that the thickness, optical parameters and elemental composition of thin films are not affected by QDs doping. The doped as-prepared thin film exhibit low intensity photoluminescence (PL) with the peak maximum at 537 nm. The PL intensity of doped samples is decreasing with increasing annealing temperature. However, luminescence of doped thin films can be significantly enhanced (3 – 10 times) by UV light exposure probably due to the photo-induced structural changes on boundary between $CdS_{0.9}Se_{0.1}$ QDs and $Ge_{25}S_{75}$ glass matrix. The photo-induced increase of PL intensity can be potentially used for local PL enhancement induced by beam of higher energies whereas the beam of lower energy would only induce the PL without changing of PL intensity.

Conflicts of interest

There are no conflicts to declare.

Acknowledgements

References

1   T. Wakaoka, K. Hirai, K. Murayama, Y. Takano, H. Takagi, S. Furukawa and S. Kitagawa, *J. Mater. Chem. C*, 2014, **2**, 7173-7175.
2   B. Rajbanshi, S. Sarkar and P. Sarkar, *J. Mater. Chem. C*, 2014, **2**, 8967-8975.
3   S. Dey, S. Chen, S. Thota, M. R. Shakil, S. L. Suib and J. Zhao, *J. Phys. Chem. C*, 2016, **120**, 20547-20554.
4   A. Marchioro, P. J. Whitham, K. E. Knowles, T. B. Kilburn, P. J. Reid and D. R. Gamelin, *J. Phys. Chem. C*, 2016, **120**, 27040-27049.
5   G. G. Yordanov, G. D. Gicheva and C. D. Dushkin, *Mater. Chem. Phys.*, 2009, **113**, 507-510.
6   K. Ersching, C. E. M. Campos, J. C. de Lima and T. A. Grandi, *Mater. Chem. Phys.*, 2008, **112**, 745-748.
7   I. L. Medintz, H. T. Uyeda, E. R. Goldman and H. Mattoussi, *Nat. Mater.*, 2005, **4**, 435-446.
8   Y. Chang, F. Pinaud, J. Antleman and S. Weiss, *J. Biophoton.*, 2008, **1**, 287-298.
9   J. Kwak, W. K. Bae, D. Lee, I. Park, J. Lim, M. Park, H. Cho, H. Woo. D. Y. Yoon, K. Char, S. Lee and C. Lee., *Nano Lett.*, 2012, **12**, 2362-2366.
10 B. Zhou, L. Tao, Y. H. Tsang and W. Jin, *J. Mater. Chem. C*, 2013, **1**, 4313-4318.
11 D. Roy, T. Routh, A. V. Asaithambi, S. Mandal and P. K. Mandal, *J. Phys. Chem. C*, 2016, **120**, 3483-3491
12 S. Sapra, A. L. Rogach and J. Feldmann, *J. Mater. Chem.*, 2006, **16**, 3391-3395.
13 D. V. Talapin, A. L. Rogach, A. Kornowski, M. Haase and H. Weller, *Nano Lett.*, 2001, **1**, 207-211.
14 J. Hambrock, A. Birkner and R. A. Fischer*, J. Mater. Chem.*, 2001, **11**, 3197-3201.
15 A. Nag, S. Sapra, S. Chakraborty, S. Basu and D. D. Sarma, *J. Nanosci. Nanotechnol.*, 2007, **7**, 1965-1968.
16 K. Tanaka and K. Shimakawa, *Amorphous Chalcogenide Semiconductors and Related Materials*, Springer, New York. 2011.
17 Z. Borisova, *Glassy Semiconductors*, Plenum Press, New York, 1981.
18 R. M. Almeida, L. F. Santos, A. Simens, A. Ganjoo and H. Jain, *J. Non-Cryst. Solids,* 2007, **18–21**, 2066-2068.
19 E. Baudet, C. Cardinaud, A. Girard, E. Rinnert and V. Nazabal, *J. Non-Cryst. Solids*, 2016, **444**, 64-72.
20 A. Stronski, M. Vlcek and A. Sklenar, *Quant. Electron. Optoelectron.,* 2000, **3**, 394-399.
21 D. H. Cha, H. Kim, Y. Hwang, J. C. Jeong and J. Kim, *Appl. Opt.*, 2012, **51**, 5649-5656.
22 T. Kanamori, Y. Terunuma, S. Takahashim and M. Miyashita, *J. Lightwave Technol.*, 1984, **2**, 607-613.
23 K. Tanaka and M. Mikami, *Phys. Status Solidi C*, 2011, **8**, 2756-2760.
24 G. Chern and I. Lauks, *J. Appl. Phys.*, 1982, **53**, 6979-6982.
25 S. Slang, K. Palka, L. Loghina, A. Kovalskiy, H. Jain and M. Vlcek, *J. Non-Cryst. Solids*, 2015, **426**, 125-131.
26 M. Waldmann, J. D. Musgraves, K. Richardson and C. B. Arnold, *J. Mater. Chem.*, 2012, **22**, 17848-17852.
27 L. Strizik, T. Wagner, V. Weissova, J. Oswald, K. Palka, L. Benes, M. Krbal, R. Jambor, C. Koughia and S. Kasap, *J. Mater. Chem. C*, 2017, DOI: 10.1039/C7TC02609A.
28 S. Novak, D. E. Johnston, C. Li, W. Deng and K. Richardson, *Thin Solid Films*, 2015, 588, 56-60.
29 K. Palka, T. Syrovy, S. Schröter, S. Brückner, M. Rothardt and M. Vlcek, Opt. Mater. Express, 2014, 4, 384-395.
30 S. Slang, K. Palka, H. Jain and M. Vlcek, *J. Non-Cryst. Solids*, 2017, **457**, 135-140.
31 S. Slang, P. Janicek, K. Palka and M. Vlcek, *Opt. Mater. Express*, 2016, **6**, 1973-1985.
32 B. O. Dabbousi, M. G. Bawendi, O. Onitsuka, and M. F. Rubner, *Appl. Phys. Lett.*, 1995, **66**, 1316-1318.
33 H. Mattoussi, L. H. Radzilowski, B. O. Dabbousi, D. E. Fogg, R. R. Schrock, E. L. Thomas, M. F. Rubner and M. G. Bawendi, *J. Appl. Phys.*, 1999, **86**, 4390-4399.
34 M. Zhu, X. Peng, Z. Wang, Z. Bai, B. Chen, Y. Wang, H. Hao, Z. Shao and H. Zhong*, J. Mater. Chem. C*, 2014, **2**, 10031-10036.
35 M. V. Kovalenko, R. D. Schaller, D. Jerzab, M. A. Loi and D. V. Talapin, *J. Am. Chem. Soc.*, 2012, **134**, 2457-2460.
36 S. Novak, L. Scarpantonio, J. Novak, M. D. Pre, A. Martucci, J. D. Musgraves, N. D. McClenaghan and K. Richardson, *Opt. Mater. Express*, 2013, **3**, 729-738.
37 N. Sultanova, S. Kasarova and I. Nikolov, *Bulg. J. Phys.*, 2013, **40**, 258-264.
38 J. Liu and M. Ueda, *J. Mater. Chem.*, 2009, **19**, 8907-8919.
39 N. Tanio and Y. Koike, *Polym. J.*, 2000, **32**, 43-50.
40 J. K. Cooper, A. M. Franco, S. Gul, C. Corrado and J. Z. Zhang, *Langmuir*, 2011, **27**, 8486-8493.
41 Q. Wang, D. C. Pan, S. C. Jiang, X. L. Ji, L. J. An and B. Z. Jiang, *Chem. Eur. J.*, 2005, **11**, 3843-3848.
42 C. Unni, D. Philip, S. L. Smitha, K. M. Nissamudeen and K. C. Gopachandran, *Spectrochim. Acta A*, 2009, **72**, 827-832.
43 Y. Jun, S. M. Lee, N. J. Kang, J. Cheon, *J. Am. Chem. Soc.,* 2001, **123**, 5150-5151.
44 B. E. Warren, *X-ray Diffraction*, Dover Publications, New York, 1990.
45 J. Cho, Y. K. Jung and J. Lee, *J. Mater. Chem.*, 2012, **22**, 10827-10833.
46 G. Chern, L. Lauks and K. H. Norian, *Thin Solid Films*, 1985, **123**, 289-296.
47 K. Palka, S. Slang, J. Buzek and M. Vlcek, *J. Non-Cryst. Solids*, 2016, **447**, 104-109.
48 R. Swanepoel, *J. Phys. E: Sci. Instrum.*, 1983, **16**, 1214-1222.
49 S. H. Wemple and M. DiDomenico, *Physical Review B*, 1971, **3**, 1338-1351.
50 J. Tauc, *Mater. Res. Bull.*, 1968, **3**, 37-46.
51 Z. Jindal and N. K. Verma, *Mater. Chem. Phys.*, 2010, **124**, 270-273.
52 N. Radychev, I. Lokteva, F. Witt, J. Kolny-Olesiak, H. Borchert, and J. Parisi, *J. Phys. Chem. C*, 2011, **115**, 14111–14122.